

Icarus
On the forced orbital plane of the Hilda asteroids
--Manuscript Draft--

Manuscript Number:	ICARUS-D-25-00191R1
Article Type:	Research paper
Keywords:	Hilda group; Orbital resonances; Asteroid dynamics
Corresponding Author:	Ian Matheson, MS The University of Arizona Tucson, AZ UNITED STATES
First Author:	Ian Matheson, MS
Order of Authors:	Ian Matheson, MS Renu Malhotra
Abstract:	Hilda-group asteroids librate in Jupiter's interior 3:2 mean motion resonance. We estimate that the Hilda group is observationally complete up to absolute magnitude ≤ 16.3 . This provides a statistically useful sample of thousands of resonant objects, all within a narrow range of semimajor axes, to compare with theoretical expectations of their orbital distribution from dynamical theory. We use von Mises-Fisher statistics to calculate the sample mean planes and mean plane uncertainties for the Hilda group and its Hilda, Schubart, and Potomac collisional subfamilies. Although Laplace-Lagrange linear secular theory is considered inapplicable within mean motion resonances, we find that the Laplace plane and the orbital plane of Jupiter are both statistically indistinguishable from the sample mean plane of the Hildas. In future work, we intend to extend this investigation to resonant populations in the Kuiper belt so as to further test the validity of Laplace-Lagrange linear secular theory for the mean planes of resonant populations.
Opposed Reviewers:	
Response to Reviewers:	Our responses to reviewers are in the attached PDF.

Response to the reviewers

Manuscript ID: ICARUS-D-25-00191

Authors' Reply: We thank the reviewers for their helpful and detailed feedback. We have revised the paper to address the reviewers' comments. Changes to the text are highlighted in the manuscript in red font. Significant revisions include the following:

- We now use von Mises-Fisher (vMF) statistics to calculate the sample mean planes and their uncertainties, but we continue to use circle-fit statistics to calculate the mean planes and mean plane uncertainties for the sets of clones. We add a summary of vMF statistics to our summary of circle-fit statistics. We demonstrate through theory and simulation that vMF statistics are an appropriate choice to describe the mean plane of the observed objects and its uncertainty, and that they are inappropriate for the mean planes of the clones. We also replace the statistics in the former Table 1, which is the current Table 2, with statistics appropriate to the vMF distribution.
- Instead of getting our list of Hilda asteroids from the Minor Planet Center and using the Nesvorný et al. (2015) list of asteroid families, we now use the recently published list of Hilda group asteroids from Vokrouhlický et al. (2025). The older list identified only the Hilda and Schubart collisional families, while the newer list identifies four more families, the largest of which is the Potomac family.
- We no longer verify the libration status of each asteroid, because the list from Vokrouhlický et al. (2025) provides the dynamically identified Hildas.
- Our previous magnitude restriction of $H \leq 15.7$ came from an observational completeness estimate by Hendler and Malhotra (2020) for the Hilda group known at that time, but now we apply Python code from Hendler and Malhotra (2020) to obtain an updated observational completeness limit of $H \leq 16.3$ for the Hilda group. This roughly doubles our sample size.
- We have significantly revised the former Figure 2, which is the current Figure 3, to make it easier to see the various reference planes and how they relate to the uncertainty intervals for the sample mean planes of the Hilda group and the collisional families. We have also refined the the former Figure 1, now Figure 2a alongside Figure 2b, to show the (a, e, i) distribution of the Hilda group and the collisional families.
- We have replaced discussion of the background objects with discussion of the entire Hilda group.
- We have split the former Section 4 into the current Section 4 and Section 5, to more clearly distinguish between an introduction to the Hilda asteroids and a discussion of their present-day mean plane. The former Section 5 is now Section 6, and it has been condensed and simplified.

Point-by-point responses to each of the reviewers' comments are given below.

Reviewer 1

This paper investigates the forced orbit plane of Hilda asteroids that librate in Jupiter's interior 3:2 mean motion resonance. The authors measure the mean planes of three Hilda subgroups (Hilda family, Schubart family, and background objects) and demonstrate that, despite being in resonance, these asteroids follow the local instantaneous Laplace plane as predicted by the Laplace-Lagrange linear secular theory. This finding is notable as this theory is conventionally considered inapplicable within mean motion resonances. Their measurements confirm that the mean planes of all Hilda subgroups are statistically indistinguishable from each other and from the predicted Laplace plane.

I believe this work should be published if the authors can address the following issues. Below are my comments:

1) The authors discovered the interesting dynamical behavior that resonant Hilda asteroids follow the Laplace plane given by linear secular theory. This is quite surprising, but the authors have not provided a clear explanation for this phenomenon. Given that Hilda asteroids are dominated by Jupiter's gravity, as evidenced by the Laplace plane being so close to Jupiter's orbital plane, I suspect the explanation may be that the nominal precession rate B is so large for Hilda asteroids and nearby non-resonant asteroids that the resonance itself does not significantly alter the forced plane. It would be helpful if the authors could report: 1) the precession rate of a Hilda asteroid, and 2) the precession rate of a nearby non-resonant asteroid, and compare these against the eigenfrequencies of the Solar System. If my understanding of this problem is correct, this should lead to an explanation of why Hilda asteroids, despite being in a mean motion resonance, follow the Laplace plane.

Authors' Reply: As we discussed in the Introduction section, in the absence of a theory for the forced plane of resonant minor planets we used the statistically significant population of known resonant asteroids (the Hildas) to measure their mean plane from their orbital data. That is to say, we look to nature to tell us. At this time, we would like to share this result from data analysis, leaving a "clear explanation" to a future theoretical analysis. The reviewer's comment stimulated us to add the following to the discussion section: "Because the Hilda group is in closer proximity to Jupiter and the other giant planets are much farther away and of lower mass, the dynamical environment can be closely approximated by the restricted three-body problem with the Sun, Jupiter, and a massless test particle. In the restricted three-body problem, the instantaneous forced plane is expected to be identical to the Jupiter plane; there is no other preferred plane around which a massless small body's orbital plane can precess. In the less restricted problem with additional planets on non-coplanar orbits, there are four possible hypotheses for the forced plane: the invariable plane, Jupiter's orbital plane (if Jupiter dominantly controls the dynamics of the resonant population), the Laplace forced plane, or one that is distinct from all of these if the mean motion resonance strongly affects the forced plane dynamics of resonant populations. Our results rule out the invariable plane as the forced plane of the Hilda group at high statistical confidence. However, the present-day observationally complete sample size cannot distinguish between the second and third of these hypotheses for three reasons: the size of the sample, its significant inclination dispersion, and the nearness of the Laplace plane to the Jupiter plane."

2) How were the Hilda and Schubart collisional families identified in previous works? If the identification involved comparing the free inclination of potential members, then they would naturally form rings with the forced pole as the center (as shown in Figure 1). In that case, what is the significance of comparing the mean planes of these collisional families with the Laplace plane, if they were identified using the Laplace plane as a reference? The authors need to provide better justification for this analysis.

Authors' Reply: We use the asteroid families identified by Vokrouhlický et al. (2025). These are found (by those authors) by numerically computing proper elements and then applying a hierarchical cluster-finding method in proper a , e , and i . The proper elements are computed by averaging osculating elements over 10 yr, constructing mean resonant elements over 10 kyr, and then averaging the mean resonant elements over 10 Myr. The asteroid families are not identified by finding rings in osculating q and p using the forced plane as a reference. Therefore, there is no circular reasoning inherent in computing the sample mean planes of the collisional families, as the reviewer's question suggests there might be.

3) For the background objects, simple arithmetic mean values are provided. I'm wondering why the authors didn't fit the background objects with the von-Mises distribution, a method they used in their previous works on Plutinos (Matheson et al. 2023).

Authors' Reply: Previously we avoided the use the von Mises distribution for two reasons. Firstly, the Hilda, Schubart and Potomac families present as annuli in the (q,p) plane, whereas the von Mises distribution is not an annular distribution (it is circularly symmetric and its density decreases monotonically with increasing angular distance from the mean direction). Secondly, we wanted to allow for an elliptical shape of the uncertainty region for the mean plane of the background population, in parallel to the circle-fit mean plane uncertainty regions in the (q,p) plane that we previously used for the Hilda and Schubart families.

However, with some numerical experimentation we are now persuaded that the von Mises distribution accurately estimates the prescribed level of uncertainty of the mean plane for annular populations as well as it does for disc-like populations with dense centers, as long as they are rotationally uniform around the mean plane. Because the observed Potomac, Hilda, and Schubart families are reasonably evenly distributed in their free longitudes of ascending node with respect to their vMF mean planes, we can straightforwardly apply the statistical calculations to all the observed families and make valid like-to-like comparisons between their mean plane uncertainty regions.

4) Section 5.1. To convince readers that individual objects follow the Laplace Plane, it would be more natural and easier to understand if the authors simply demonstrated the conservation of free inclination for individual Hilda objects (as shown in Figure 2 of Huang et al., 2022). The authors' method is valid but perhaps unnecessarily complex for this purpose.

Authors' Reply: We respectfully submit that our method is appropriate for the following reasons. The conservation of free inclination is neither a necessary nor a sufficient condition to demonstrate that an individual object follows the Laplace plane over time. For non-resonant Kuiper belt objects, Huang et al (2022) found that the "free inclination" measured relative to the Laplace plane shows significant variations, with deviations of more than ten degrees over a period of about 2 Myr. To find a constant free inclination, Huang et al. (2022) carried out a more complex calculation by employing a double-averaged Hamiltonian model. Their approach calculates the conserved quantities that they call "free inclinations". Notably, their approach does not aim to identify the mean plane of groups of objects nor the forced plane for individual objects; indeed Huang et al. do not report any measurements of the mean or forced planes, so we cannot know that the reported "free inclination" is actually relative to the Laplace plane or a conserved quantity that bears a more complicated relationship to the Laplace plane. In some contrast with Huang et al., we note that Volk & Malhotra (2017) and Matheson & Malhotra (2023) found that the mean planes of (non-resonant) objects in various semimajor axis intervals of the Kuiper belt are statistically compatible with treating the instantaneous Laplace plane as the true

mean plane. In the former section 5.1, we employed a relatively straightforward approach that aims to elucidate the dynamics of the forced plane of three individual Hilda group asteroids by using clones to examine the time evolution of their orbit planes; we do not address the question of conserved quantities such as “free inclinations” as defined in Huang et al. The discussion of the mean planes of the clones is now in section 6.

5) Section 5.2. If individual objects track the Laplace Plane, then group mean planes would naturally track the Laplace Plane as well. In my opinion, it would be more straightforward to demonstrate this by showing the conservation of free inclinations for the group of Hilda objects.

Authors’ Reply: The reviewer makes a simple intuitive point, but please see our response to the previous comment. By presenting the mean-plane statistics of the observed collisional families in the Hilda group, we test intuition with observational data. Due to the lack of theory for the expected mean plane of a resonant population, we used the most intuitively plausible expectation (the Laplace plane or Jupiter’s plane or the invariable plane) as a foil for our observational data-based analysis of the present-day mean plane.

6) Line 25 is missing a comma after “section 2”.

Authors’ Reply: We’ve fixed that in the appropriate line of the revision.

7) It would be nice to show Figure 1 and 2 side by side, with the scale of Figure 2 correctly marked on Figure 1. Figure 2 was confusing for me until I noticed that its plotting scale is different from Figure 1’s.

Authors’ Reply: In the revision, the former Figure 1 is now Figure 2b and the former Figure 2 is now Figure 3. We have added Figure 2a to give more information about the orbital elements of the Hilda group and we have expanded Figure 3 to make it more readable. We have added a note to the caption of Figure 3 to clarify that its scale is much smaller than the scale of Figure 2b, but we do not think it is necessary to impose an outline of Figure 3 on Figure 2b in order to communicate the relative scale.

Reviewer 2

The paper endeavors to identify the forced orbital plane of the Hilda population of asteroids in the 3:2 resonance with Jupiter. Specifically, the authors test whether the forced orbital plane at 4 au computed from the equations of Lagrange-Laplace secular theory tracks the evolution of the Hilda’s mean plane. To compute the mean plane of the actual Hilda’s, and simulated version of them, the paper makes use of Gaussian statistics and a least squares circle fit. The authors conclude that all 3 derived mean planes (those of 2 known collisional families in the population as well as the background objects) closely coincide with the instantaneous Laplace plane - which is computed via the Laplace-Lagrange equations using the osculated planet orbits at the current epoch - and Jupiter’s orbital pole. The authors also perform a series of simulations of both the actual Hildas, as well as clones of individual objects, to show that the objects continue to follow both the Lagrange plane and Jupiter’s pole forward in time. This result contradicts the common view that secular theory is not applicable inside of mean motion resonances. I think this is a novel, important addition to the literature, and merits publication in Icarus. The arguments are straightforward and

the methodology is appropriate and correctly applied. I have a number of mostly minor comments. In particular, I think the authors should include a few more relevant references, make some modest improvements to the way in which the results are presented, and expand on the discussion of the implication of the results. Specific comments follow:

1) I think the introduction should at least mention where the population is thought to have originated from (i.e. capture in the region after it was emptied by the instability: Franklin et al 2004; Vokrouhlicky et al. 2016), and what it is made up of (P- and D- types, see Dahlgren et al. 1997, Wong et al. 2017, Wong & Brown 2017.). I think this context is important for a comprehensive interpretation of the results of this paper.

Authors' Reply: This is a reasonable suggestion. We have added a paragraph to the current Section 1 to provide this context.

2) I suspect the authors submitted their paper before Vokrouhlicky et al. 2025 (<https://ui.adsabs.harvard.edu/abs/2025arXiv250304403V/abstract>) came on Arxiv. I think that a discussion of that paper, in particular its conclusions on the debiased orbital distribution of the Hildas and derived uncertainties (e.g. their figure 14 and table 2) needs to be added to the introduction and discussion sections of this paper.

Authors' Reply: The reviewer is correct that we submitted our paper before Vokrouhlicky et al 2025 was published. Rather than adding a textual discussion of this paper as it relates to our results in the first manuscript submission, we decided to redo our calculations using the lists of Hilda-group asteroids and their collisional families that they provide in their Zenodo dataset. By doing so, we now have collisional family lists that are up-to-date with the overall list of Hilda-group asteroids, thus implicitly incorporating their work on the debiased distribution of the Hildas. This means that our observational samples were revised and the mean plane estimates were also revised.

3) Line 83: "Accordngly"

Authors' Reply: We corrected this typo in the revision.

4) Line 168: I feel like this first and second paragraphs here are a little distracting. The information itself is fine to include if you like, but isn't the point you want to make that the Hilda population represents the best (i.e most observationally constrained resonant populations) for your analysis? I think this section should lead off with this as a strong statement, and this point should also be made in the introduction as well.

Authors' Reply: We did make this point in the current Section 1, to wit: "The Hilda asteroids, librating in Jupiter's interior 2:3 MMR, represent a statistically significant sample of nearly 4000 objects which is observationally complete to $H \leq 16.3$, so we can use them as a test case to investigate their mean orbital plane while limiting our uncertainties to those inherent in the sample statistics without concern for observational survey biases." However, we can see how we buried the lede in this section, so we rewrote the first two paragraphs of the current Section 4 to lead off with a strong statement, as suggested.

5) Line 185: What is the timescale for turning an arc into a circle in the Hilda region? I'd suspect fairly short. A quick back-of-the-envelope estimate would be useful here, or something derived from the simulations in section 5.

Authors' Reply: The timescale for turning an arc into a circle depends inversely on the initial semimajor axis dispersion (assuming a very small dispersion, typical of collisional families). For an initial dispersion of ± 0.01 au, we determined from our integrations of Potomac, Hilda, Schubart, and Ismene clones that this timescale for Hilda-group asteroids is several hundred kyr to about 1 Myr. We have added text at the end of the current Section 4 to address this point.

6) Line 187: I think you should at least cite Broz & Vokrouhlicky 2011 here, who identified the Hilda group as containing 2 families. Schubart 1982 and 1991 are relevant as well.

Authors' Reply: We have added references to these three papers at this point in the manuscript (the second paragraph of the current Section 4).

7) Figure 1: I think a little more context in the first figure would help the paper. Perhaps an additional panel showing proper a vs. inc of the Hilda region with 5 colors: All background objects in the region, Hildas discarded from analysis in this paper (3) Background Hildas used in this paper, (4-5) Hilda and Schubart family members used in this paper. The authors can feel free to take or leave my suggestion.

Authors' Reply: With the revised Vokrouhlický et al. (2025) dataset, the number of circulating objects in our calculations was small and excluding them resulted in negligible changes to the mean plane and mean plane calculations. Accordingly, we do not discuss checking the 3:2 resonant angle in the revision. As suggested by the reviewer, we have added a set of scatter plots of the orbital elements, a, e, i , as the current Figure 2a. We plot osculating heliocentric elements, as these are pertinent to our investigation of the mean plane. The (a, i) plot shows that the semimajor axes of the collisional families are randomly distributed across their ranges, and the (a, e) plot shows that semimajor axis and eccentricity are uncorrelated.

8) Section 4: I think the last two paragraphs should be flipped.

Authors' Reply: The location of that content in the revised paper is at the end of Section 5. We did not flip the order of the last two paragraphs in the revision, because the discussion of the statistical overlap of various mean planes follows naturally from the immediately preceding presentation of what the subplots of Figure 3 represent. The numerical value of the mean plane of the entire Hilda group is then presented in the concluding paragraph of section 5. This complements the discussion of the uncertainty region half-angles in the preceding paragraph.

9) End of Section 5.1: It would also be useful to remind the reader here that the instantaneous Laplace plane is calculated with the simulated osculating elements of the planets. So, the calculation here uses just the giant planets, correct? Whereas the calculation in section 4 uses all 8 presumably? Not that it would matter, I just think it's worth clarifying.

Authors' Reply: We now state explicitly in section 2 that we always calculate the Laplace plane using the instantaneous heliocentric osculating orbital elements of only the outer planets Jupiter, Saturn, Uranus, and Neptune.

10) Section 5.2: I was confused when I started reading this it seemed like you were still talking about the clones. It might help to just say that these are the "actual" objects in the first sentence.

Authors' Reply: We hope the revised discussion of this content in the current Section 6 is more clear.

11) Figure 3: Similarly, it would help if rows 1&2 were flipped with 3&4, as they come first in the text, alternatively, you could just add something like "top 2 rows" and "bottom 2 rows" to the in-text citation to figure 3 in 5.1 and 5.2.

Authors' Reply: We've altered Figure 3 to be more readable and we've added clarifying language to the in-text citations.

12) Conclusions: The result here is indeed surprising. I understand that the authors plan to continue to explore this topic in future work, but I do feel that a bit more could be said in this paper. In particular, it would be useful for the authors to comment on whether this outcome would be universally applicable to any resonant population of small bodies (or rather, why it is not), a result of something specific to the Hilda populations' particular orbital distribution, or something specific to the resonance itself. I would be curious if the author's results would change, and if so by how much, if, for example, they altered the underlying inclination distribution of the Hildas, or if they created a synthetic population of resonators in a different resonance.

Authors' Reply: The fifth paragraph in the revised Section 7 is a qualitative explanation for our result, but it is specific to the Hilda group as a population in an environment very closely approximated by the restricted three-body problem and may not generalize to other mean motion resonances. The last two paragraphs in Section 7 discuss what we see as the main weaknesses in our study and the most promising avenues of future study on the topic of the forced planes of resonant small-body populations.

13) Section 7: The GitHub link did not work for me.

Authors' Reply: We hadn't put anything up on GitHub at the time we submitted our manuscript (as noted previously). With this revision, we have now uploaded our Python scripts and pertinent data files to GitHub, as noted in the revised Data Availability statement.

Very interesting work.

Best wishes,

Matt Clement

References

- Hendler, N.P., Malhotra, R., 2020. Observational completion limit of minor planets from the asteroid belt to jupiter trojans. *The Planetary Science Journal* 1, 75.
- Nesvorný, D., Brož, M., Carruba, V., et al., 2015. Identification and dynamical properties of asteroid families. *Asteroids IV* 29, 7–321.
- Vokrouhlický, D., Nesvorný, D., Brož, M., Bottke, W.F., Deienno, R., Fuls, C.D., Shelly, F.C., 2025. Orbital and absolute magnitude distribution of hilda population. *The Astronomical Journal* 169, 242.

Highlights

On the forced orbital plane of the Hilda asteroids

Ian C. Matheson, Renu Malhotra

- We measure the mean **orbital** planes of the Hilda group asteroids and their collisional subfamilies.
- The mean planes of the Hildas and their sub**families** are all **statistically indistinguishable from Jupiter's orbital plane and from the Laplace plane defined by linear secular theory**.
- We rule out the invariable plane as the mean **orbital** plane of the Hildas.

Declaration of Interest Statement

- The authors declare that they have no known competing financial interests or personal relationships that could have appeared to influence the work reported in this paper.
- The author is an Editorial Board Member/Editor-in-Chief/Associate Editor/Guest Editor for this journal and was not involved in the editorial review or the decision to publish this article.
- The authors declare the following financial interests/personal relationships which may be considered as potential competing interests:

Highlights

On the forced orbital plane of the Hilda asteroids

Ian C. Matheson, Renu Malhotra

- We measure the mean **orbital** planes of the Hilda group asteroids and their collisional subfamilies.
- The mean planes of the Hildas and their sub**families** are all **statistically indistinguishable from Jupiter's orbital plane and from the Laplace plane defined by linear secular theory**.
- We rule out the invariable plane as the mean **orbital** plane of the Hildas.

On the forced orbital plane of the Hilda asteroids

Ian C. Matheson^{a,*}, Renu Malhotra^b

^aDepartment of Aerospace and Mechanical Engineering, The University of Arizona, 1130 N. Mountain Ave., P.O. Box 210119, Tucson, 85721, AZ, USA

^bLunar and Planetary Laboratory, The University of Arizona, 1629 E. University Blvd., Tucson, 85721, AZ, USA

ARTICLE INFO

Keywords:

Hilda group
Orbital resonances
Asteroid dynamics

ABSTRACT

Hilda-group asteroids librate in Jupiter's interior 3:2 mean motion resonance. We estimate that the Hilda group is observationally complete up to absolute magnitude $H \leq 16.3$. This provides a statistically useful sample of thousands of resonant objects, all within a narrow range of semi-major axes, to compare with theoretical expectations of their orbital distribution from dynamical theory. We use von Mises-Fisher statistics to calculate the sample mean planes and mean plane uncertainties for the Hilda group and its Hilda, Schubart, and Potomac collisional subfamilies. Although Laplace-Lagrange linear secular theory is considered inapplicable within mean motion resonances, we find that the Laplace plane and the orbital plane of Jupiter are both statistically indistinguishable from the sample mean plane of the Hildas. In future work, we intend to extend this investigation to resonant populations in the Kuiper belt so as to further test the validity of Laplace-Lagrange linear secular theory for the mean planes of resonant populations.

1. Introduction

The mean orbital plane of groups of small bodies in the solar system is understood to be forced by the secular gravitational perturbations of the major planets. For small bodies in the solar system that are not subject to a planetary mean motion resonance (MMR), the Laplace-Lagrange linear secular theory provides an estimate of the forced orbital plane as a function of semi-major axis, when the small body is treated as a massless test particle (Murray and Dermott, 1999). For a group of non-resonant small bodies with a small dispersion in semimajor axis, their average forced plane according to linear secular theory provides an excellent theoretical estimate of their mean orbital plane (Chiang and Choi, 2008; Volk and Malhotra, 2017; Matheson and Malhotra, 2023).

In the present work, we ask: what is the forced orbital plane of dynamical groups of resonant small bodies? The Laplace-Lagrange secular theory is ostensibly not applicable in MMR zones, as the resonant terms in the disturbing function are omitted from its derivation, as in Murray and Dermott (1999, chapters 6-7), although this limitation is not well defined. Typical textbook reviews of resonant small-body behavior, as in Murray and Dermott (1999, chapter 8), focus on the coplanar case and omit out-of-plane motion. The literature on out-of-plane motion of small bodies near mean motion resonances appears to be silent on the forced plane and focuses on the determination of the “proper inclination” as one of the quasi-integrals that are nearly time-invariant in the long term dynamics of small bodies (e.g. Knezevic, Lemaître and Milani, 2002; Nesvorný, Roig, Vokrouhlický and Brož, 2024).

Here we probe the question of the forced plane of a group of small bodies librating in a mean motion resonance. We use observational data and numerical simulation as the most convenient means of studying this question. The Hilda asteroids, librating in Jupiter's interior 3:2 MMR, represent a statistically significant sample of nearly 4000 objects which is observationally complete to absolute magnitude $H \leq 16.3$ (see Section 4), so we can use them as a test case to investigate their mean orbital plane while limiting our uncertainties to those inherent in the sample statistics without concern for observational survey biases. With this large observational sample, we test the hypothesis that the mean plane of this resonant group of asteroids is given by the forced plane defined by the Laplace-Lagrange secular theory. We also discuss the invariable plane and Jupiter's orbital plane as possible forced planes.

Previous studies of the Hilda asteroids have measured their reflectance spectra, finding a correlation between magnitude and surface composition (mainly D- and P-type) in the Hilda group (Dahlgren, Lagerkvist, Fitzsimmons, Williams and Gordon, 1997) that suggests (Wong and Brown, 2017; Wong, Brown and Emery, 2017) a possible common origin with the Jupiter trojans, which have a remarkably similar magnitude-color distribution. Franklin,

*Corresponding author

✉ ianmatheson@arizona.edu (I.C. Matheson)

ORCID(s): 0000-0003-0940-7176 (I.C. Matheson); 0000-0002-1226-3305 (R. Malhotra)

Lewis, Soper and Holman (2004) argued that the eccentricity distribution of the observed Hildas is evidence that this primordial population was swept up in Jupiter's interior 3:2 MMR as Jupiter migrated inward. Brož, Vokrouhlický, Morbidelli, Nesvorný and Bottke (2011) add the requirement for this migration to take place during the Late Heavy Bombardment, in a system with an extra giant planet (later ejected), and with a substantial YORP effect. Further extending this line of reasoning, Vokrouhlický, Bottke and Nesvorný (2016) suggested that the primordial Hilda and Trojan populations were interlopers from the trans-Neptunian region injected inward by the giant planet instability, and that their subsequent depletion has been largely driven by the YORP mechanism. These holistic studies of long-term Hilda evolution are fairly successful in accounting for the observed composition, size, and eccentricity distributions of the Hilda group asteroids, but these studies have not addressed the relatively simple question of what the forced plane of this resonant population might be.

We present the results of our investigation by organizing the rest of this paper as follows.

- In section 2, we provide a brief description of the Laplace-Lagrange linear secular theory for the forced plane of a minor planet. This provides theoretical context for the analysis of the observational data.
- In section 3, we briefly describe the von Mises-Fisher (vMF) distribution, which forms the basis of our calculations of the mean plane and its uncertainty, and we justify its application to the mean orbital plane of the Hilda asteroids. We also describe the statistical method we use to find the mean plane and mean plane uncertainty for the sets of asteroid clones in Section 6.
- In section 4, we present our sample of Hilda-group asteroids and the collisional families within.
- In section 5, we show the present-day mean plane of the Hilda group and its collisional families, and we comment on its relation to the forced plane, the orbital plane of Jupiter, and the invariable plane of the Solar System.
- In section 6, we comment on the motion of the mean plane over time in relation to the forced plane, for the observed Hilda asteroids and for sets of clones of selected individual asteroids.
- Section 7 provides discussion and summary of our work.

2. Laplace-Lagrange Linear Secular Theory

In sections 5-6, we will compute the mean plane of the observed Hilda-group asteroids at the present time, then simulate the orbits of the Hildas for several Myr and compute their mean plane over that time. This section outlines the dynamical theory we will use to interpret the present-day observed mean plane and the computed mean plane in the future.

Laplace-Lagrange linear secular theory is a simplified description of the secular dynamics of massive planets and massless small bodies obtained by expanding the disturbing function to low order and discarding short-period and resonant terms. This summary of the theory follows Murray and Dermott (1999, chapter 7).

The simplified physical model is that of a single small body, represented as a massless point, and N point-mass planets orbiting a point-mass Sun, ignoring the collective gravitational effects of a massive disk of small particles. The orbits of the small body and each massive planet are given as heliocentric osculating elements. The disturbing function for the small body as well as of the planets is expanded to first order in the masses, second order in the eccentricities, and second order in the inclinations. Short-period and resonant terms are discarded, leaving only the secular terms of the direct part of the disturbing function, as the indirect part has no secular terms. The absence of resonant terms then implies that the semimajor axes are constant in time.

It is convenient to rewrite the disturbing function as a quadratic form in the variables $h = e \sin \varphi$, $k = e \cos \varphi$, $p = \sin i \sin \Omega$, and $q = \sin i \cos \Omega$. Here e , φ , i , and Ω respectively denote the orbital eccentricity, the longitude of perihelion, the orbital inclination and the longitude of ascending node; the standard reference plane is the J2000 ecliptic. In this paper, we refer to Ω as simply the “ascending node”. The lowest-order formulations of Lagrange's equations of motion for h , k , q , and p for each planet and for the small body then become a system of coupled first order linear differential equations with constant coefficient matrices that couple k with h and q with p , while leaving (k, h) uncoupled from (q, p) . Because the orbital planes are fully described by q and p , we will omit further discussion of k and h .

75 The orientation of the plane of a Keplerian orbit is given by the unit vector $\hat{\mathbf{h}}$ pointing in the direction of the orbital
 76 angular momentum vector, given by

$$\hat{\mathbf{h}} = (h_x, h_y, h_z) = (\sin i \sin \Omega, -\sin i \cos \Omega, \cos i), \quad (1)$$

77 which depends only on i and Ω , or in other words on q and p . For convenience, we prefer to express the orbital plane
 78 as a unit vector $\hat{\mathbf{q}}$ on the surface of the unit sphere where

$$\hat{\mathbf{q}} = (-h_y, h_x, h_z) = (q, p, s) = (\sin i \cos \Omega, \sin i \sin \Omega, \cos i). \quad (2)$$

79
 80 The coupled first-order linear differential equations in q and p can be solved to find $\mathbf{q} = (q, p)$ as a function of time
 81 for the small body and for each of the planets. For each planet, the solution is a superposition of N linear modes, one
 82 of which has zero frequency and is identified with the invariable plane of the Solar System (the plane normal to the
 83 total barycentric orbital angular momentum vector). For the small body, the solution is given by the sum of a “free
 84 plane” $\mathbf{q}_1 = (q_1, p_1)$ and a “forced plane” $\mathbf{q}_0 = (q_0, p_0)$. The free plane \mathbf{q}_1 precesses at a fixed rate B around the forced
 85 plane \mathbf{q}_0 , which is itself a weighted superposition of the linear modes of the orbital planes of the planets. Note that \mathbf{q}_0
 86 is defined in Laplace-Lagrange linear secular theory as the forced plane for a small body at a specific semimajor axis,
 87 and henceforth we will call it the “Laplace plane”. The total orbital plane $\mathbf{q} = (q, p)$ is given by Murray and Dermott
 88 (1999, eq. 7.146):

$$q = q_1(t) + q_0(t) = \sin i_{\text{free}} \cos(Bt + \gamma) + q_0(t), \quad (3)$$

$$p = p_1(t) + p_0(t) = \sin i_{\text{free}} \sin(Bt + \gamma) + p_0(t). \quad (4)$$

89 In this expression, the free inclination i_{free} and phase γ are constants computed from the initial conditions of the
 90 planetary and small-body orbits, and the frequency B is computed from the masses and (constant) semimajor axes of
 91 the planets. The forced plane $\mathbf{q}_0 = (q_0, p_0)$ is given by Murray and Dermott (1999, eq. 7.149-7.150):

$$q_0(t) = - \sum_{i=1}^N \frac{\mu_i}{B - f_i} \cos(f_i t + \gamma_i), \quad (5)$$

$$p_0(t) = - \sum_{i=1}^N \frac{\mu_i}{B - f_i} \sin(f_i t + \gamma_i). \quad (6)$$

92 The frequencies f_i and the amplitudes μ_i come from the eigenvalues and eigenvectors, respectively, of the coefficient
 93 matrices in the coupled differential equations for q and p . The elements of the coefficient matrices are computed from
 94 the masses of the planets and from their osculating semimajor axes, inclinations, and ascending nodes. These are
 95 the same frequencies and amplitudes as are found in the linear modes of the linear secular solutions for the planets.
 96 The phases γ_i are found from the initial conditions. In a more accurate model, such as in a full multi-body numerical
 97 simulation, the quantities B , μ_i , f_i , and γ_i all vary slowly, but they are constant in Laplace-Lagrange linear secular
 98 theory. For the purposes of the present investigation, their variation may be neglected over timescales of several Myr.

99 When speaking of the Laplace plane, we note that the constant parameters in Eqs. 3–6 are calculated for some
 100 epoch $t = 0$. We therefore distinguish the “propagated Laplace plane”, calculated at some time $t = \tau$ from the
 101 osculating orbits of the planets at the epoch $t = 0$ and setting $t = \tau$ in Eq. 5–6, from the “instantaneous Laplace
 102 plane”, calculated at $t = \tau$ from the heliocentric osculating orbits of the planets at $t = \tau$ in a multi-body numerical
 103 simulation and setting $t = 0$ in Eq. 5–6. In other words, for the propagated Laplace plane, the constants in Eq. 5–6
 104 are calculated from the heliocentric osculating orbital elements at some epoch $t = 0$, and are constant only within
 105 the approximations of linear secular theory. When comparing theory with full multi-body numerical simulations, we
 106 recognize that the semimajor axes of the planets and the constants in Eq. 5–6 do not in fact remain constant, so we
 107 calculate the instantaneous Laplace plane using the instantaneous osculating orbital elements of the massive planets and
 108 the instantaneous heliocentric osculating semimajor axis of the minor planet.. Accordingly, the calculations, figures,
 109 and tables in this paper exclusively use the instantaneous Laplace plane, not the propagated Laplace plane. It is also
 110 important to note that we calculate the instantaneous Laplace plane using the instantaneous heliocentric osculating
 111 orbital elements of only the outer planets Jupiter, Saturn, Uranus, and Neptune, neglecting perturbations from the

inner planets Mercury, Venus, Earth, and Mars. Instead, we add the inner planet masses to the mass of the Sun and decrease the outer planet mass ratios relative to the Sun proportionally.

A small body's Laplace plane depends only on its semimajor axis, not on the other elements of its orbit. Therefore, as shown in theory and simulation by Chiang and Choi (2008), linear secular theory makes a simple and testable prediction for the mean orbital plane of a group of massless small bodies under the condition that the object have similar semimajor axes. Objects with slightly different semimajor axes will precess around nearby, but not identical, Laplace planes at slightly different rates. Given enough time, their orbital planes form a thin ring in q and p . The forced orbital plane of the objects considered as a group may be identified with the Laplace plane of some appropriate statistical measure of their central semimajor axis, and the mean orbital plane may be identified with some appropriate statistical measure of the center of the orbital planes in q and p . The mean orbital plane should, to within some measure of statistical confidence, coincide with the forced plane of the Laplace-Lagrange theory at the central semimajor axis.

Laplace-Lagrange linear secular theory produces a well-defined forced plane for most semimajor axis locations, but it must be used with caution. The f_i frequencies are fixed by the planets' parameters, while the B frequency depends both on the planets' parameters as well as on the semimajor axis of the massless small body. When $B - f_i \rightarrow 0$, the coefficients of the i th terms of q_0 and p_0 (Eq. 5–6) grow without bound, and the forced plane has an unbounded inclination (in the linear approximation). These singularities are known as "secular resonances", and must be analyzed using a higher-order theory to resolve the singularities; the first-order results are of limited accuracy near these secular resonances. Secular resonances have actually been identified to exist in narrow regions inside Jupiter's 3:2 MMR (e.g., Morbidelli, 1993; Ferraz-Mello, Michtchenko, Nesvorný, Roig and Simula, 1998). However, the real Hilda asteroids are absent from these regions and are unaffected by these secular resonances (Morbidelli and Moons, 1993; Zain, Di Sisto and Gil-Hutton, 2025; Nesvorný and Ferraz-Mello, 1997), so we do not address them further in this paper.

Furthermore, as we noted in section 1, because the first step in the derivation of linear secular theory is the discarding of resonant terms from the disturbing function, the theory is not constructed to be applicable to massless small bodies located in planetary MMRs, and it must certainly be applied with caution nearby. Nevertheless, in the absence of an alternative, the Laplace-Lagrange theory is useful in our investigation as a comparison for the measured mean plane of the observed Hilda asteroids.

3. Statistics of the Mean plane

For an observationally complete sample of a group of n minor planets, their mean plane and its measurement uncertainty can be estimated with a relatively simple statistical approach. Estimating the uncertainty of the mean plane requires the greater effort, which we detail in this section. Let us assume that the orbital planes of a group of n minor planets, described by their (q_i, p_i) values, form an approximately circular disk in the (q, p) plane, or an annulus of some average radius and narrow width, or an arc of such an annulus. In the disk and annular cases, we treat the orbital planes as unit vectors and apply von Mises-Fisher statistics on the unit sphere to find the mean plane and its uncertainty. We outline these statistics in Section 3.1. For the circular arc case, we use a circle-fitting algorithm to find the center and radius of the best-fit circle. We outline the circle-fitting algorithm and its uncertainty in Section 3.2.

3.1. The von Mises-Fisher Distribution

The von Mises-Fisher distribution is the simplest analogue of the Gaussian normal distribution on the unit sphere. The probability density function is given by

$$f(\hat{\mathbf{q}}; \hat{\mu}, \kappa) = \frac{\kappa}{4\pi \sinh \kappa} \exp(\kappa \hat{\mathbf{q}}_0^T \hat{\mathbf{q}}), \quad (7)$$

where $\hat{\mathbf{q}}$ is the full unit vector for the orbit plane, $\hat{\mathbf{q}}_0$ is the unit vector for the mean plane, and $\kappa > 0$ is the concentration parameter. The vMF distribution is rotationally uniform around $\hat{\mathbf{q}}_0$. Larger values of κ result in distributions that are more highly concentrated around the mean direction. The mean direction $\tilde{\hat{\mathbf{q}}}_0$ of a sample of n orbital planes $\hat{\mathbf{q}}_i$, $i = 1, \dots, n$, is found by adding up the $\hat{\mathbf{q}}_i$ and normalizing to the unit sphere. The uncertainty in the sample mean direction $\tilde{\hat{\mathbf{q}}}_0$ is described by small circles on the unit sphere centered on $\tilde{\hat{\mathbf{q}}}_0$. The angular width $\phi_{95\%}$ that encloses 95% of the probability mass in the sampling distribution for $\tilde{\hat{\mathbf{q}}}_0$ is calculated as described in Matheson, Malhotra and Keane (2023).

It should be understood that when the sample mean pole is $\hat{\mathbf{k}} = (0, 0, 1)$, the projection of the mean plane uncertainty circle on the (q, p) plane is precisely circular, but if the inclination of the sample mean pole is nonzero, this circle will

Category	<i>n</i>	68%	95%	99.7%
All Hildas	3893	0.68125	0.94957	0.99693
Schubart family	983	0.68062	0.95009	0.99669
Hilda family	737	0.68013	0.94803	0.9967
Potomac family	359	0.68031	0.94964	0.99682

Table 1

Columns are category; object count ($H \leq 16.3$); and proportion of bootstrap samples with vMF sample 68%, 95%, and 99.7% uncertainty regions that enclose the true mean plane of the model population, $\hat{\mathbf{k}}$.

be compressed in the radial direction and form an ellipse. For low mean inclinations, the eccentricity of this ellipse is small and we neglect it. In this approximation, the mean plane uncertainties in q , p , i , and Ω are all equal to σ . That is, using vMF statistics and for low inclination mean poles, $\sigma_i \approx \sigma_\Omega \approx \sigma_q \approx \sigma_p \equiv \sigma$. In the flat plane approximation, σ_q and σ_p quantify the uncertainty in the location of the mean pole in the horizontal and vertical q and p directions, while σ_i quantifies that uncertainty in the radial direction relative to the ecliptic pole and σ_Ω quantifies it in the transverse direction. Because the vMF uncertainty region is effectively a circle, σ_q , σ_p , σ_i , and σ_Ω all measure its diameter in different directions and are all equal.

The orbital planes of the Hilda-group asteroids appear rotationally uniform relative to their sample mean plane, but their distribution differs from a vMF distribution (cf. Figure 1 and Figure 2b). A substantial “background” population does resemble a vMF distribution, but the collisional families present as separate concentric thin rings. Neither the thin rings of the collisional families, nor the Hilda group as a whole, can plausibly be called a vMF distribution. Nevertheless, we make the ansatz that the sampling distribution of the mean plane does, based on the following reasoning.

First, note that the vMF distribution is obtained by restricting the isotropic uncorrelated trivariate Gaussian distribution to the surface of the unit sphere and recalculating the normalizing coefficient.

Because of this, it is intuitive that the sampling distribution for the mean direction of rotationally uniform distributions on the unit sphere should converge to the vMF distribution, just as the central limit theorem guarantees that the sampling distribution for the mean of general trivariate distributions converges to the Gaussian distribution. We do not prove this, but we demonstrate it for a few distributions relevant to this work.

As discussed later in section 4, the Hilda-group asteroids contain three large collisional families, named after the asteroids Hilda, Schubart, and Potomac. In this paper, we call the collisional family named for asteroid Hilda the “Hilda family”, while we call the entire population of 3:2 resonant asteroids the “Hilda group”. Those Hilda-group asteroids not associated with any collisional family will be referred to as the “background Hildas”. The orbital planes of the Hilda family form a thin ring on the unit sphere with an inclination width of about 9° . The orbital planes of the Schubart and Potomac families form thin rings with inclination widths of about 3° and 11° . The orbital planes of the background Hildas more closely resemble a classic vMF distribution.

To show that the vMF distribution adequately describes the sampling distribution for the mean of each family and of the entire Hilda group, we construct model populations by first computing the vMF mean plane $\hat{\mathbf{q}}_0$ of each sample and then computing the inclination for each object in the sample relative to the sample mean. We draw 100,000 bootstrap samples of relative inclination, pair them with equally sized uniform random samples on the circle for the ascending node, and construct unit vectors. Next, we compute the vMF sample mean and $\phi_{68\%}$, $\phi_{95\%}$, and $\phi_{99.7\%}$ for each bootstrap sample of unit vectors. We record how many times the true mean plane $\hat{\mathbf{k}} = (0, 0, 1)$ is within the 68%, 95%, and 99.7% uncertainty regions. If the vMF distribution is a suitable description of the sampling distribution of the mean of an arbitrary rotationally uniform distribution on the unit sphere, then the proportion of the time that the true mean plane is within a given uncertainty region should be very close to the percentage prescribed for that uncertainty region.

In Figure 1, we show histograms of the empirical relative inclination distributions of the Schubart, Hilda, and Potomac collisional families from which our bootstrap samples are drawn, and for the entire Hilda group. In Table 1, we show what proportion of bootstrap sample repetitions yielded sample mean uncertainty regions that enclosed the true mean plane $\hat{\mathbf{k}}$. These proportions closely match the specified uncertainty levels, showing the vMF distribution to adequately model the distribution of the sample mean for rotationally symmetric samples resembling the orbital planes of the Hilda-group asteroids. In other words, we have demonstrated that the mean plane obeys vMF statistics even when the sample itself does not, provided the sample is rotationally symmetric.

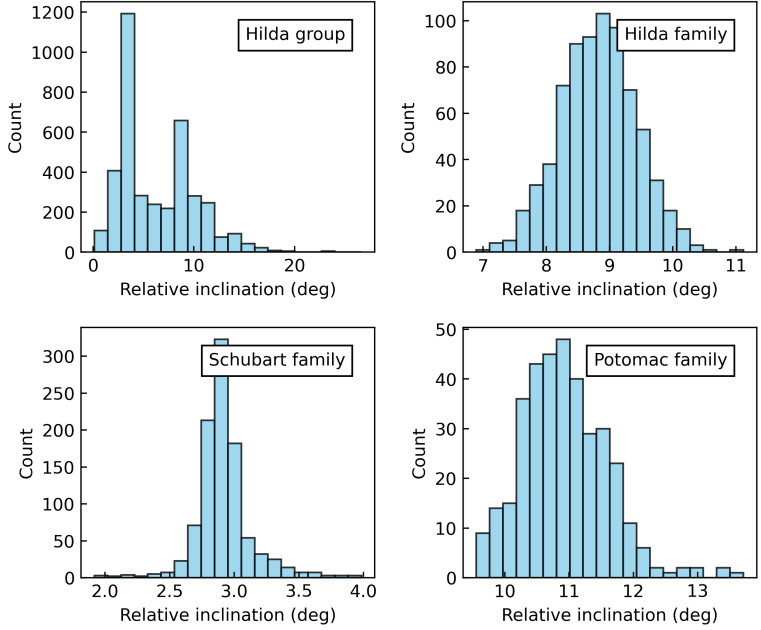


Figure 1: Histograms for the inclinations of the Hilda group, and the Schubart, Hilda, and Potomac collisional families, relative to the vMF mean plane for each population.

3.2. The Circle-Fit Mean Plane

When the orbital planes of the individual objects form one or more circular arcs in (q, p) without uniformly filling an annulus, it is necessary to use a circle-fitting algorithm to find the center and radius of the best-fit circle. (We will need this in Section 6 where we employ clones of individual asteroids to investigate the time evolution of their orbital planes.) There are a variety of circle-fitting algorithms of varying accuracy and stability for short arcs, but for long enough arcs a simple least-squares fit is sufficient. The Python package `circle-fit` (Klearn and Lauritzen, 2023) implements several circle-fitting methods from Al-Sharadqah and Chernov (2009), but does not compute the covariance matrix for any of them. We used `circle-fit` to find the center and radius of each best-fit circle, but we wrote our own Python code to compute its covariance, again following the procedures outlined in Al-Sharadqah and Chernov (2009), which we reproduce below. Our code is available on GitHub as described in section 8.

The least-squares circle fit adopts an idealized statistical model in which a model population lies exactly on a circle of center $(\tilde{q}_0, \tilde{p}_0)$ and radius \tilde{R} . The n objects in the model population have model orbital planes $(\tilde{q}_i, \tilde{p}_i)$, related to the model center by

$$\tilde{q}_i = \tilde{q}_0 + \tilde{R} \cos \tilde{\phi}_i, \quad (8)$$

$$\tilde{p}_i = \tilde{p}_0 + \tilde{R} \sin \tilde{\phi}_i \quad (9)$$

for some angle $\tilde{\phi}_i$. For later convenience, we write

$$\tilde{u}_i = \cos \tilde{\phi}_i = \frac{\tilde{q}_i - \tilde{q}_0}{\tilde{R}}, \quad (10)$$

$$\tilde{v}_i = \sin \tilde{\phi}_i = \frac{\tilde{p}_i - \tilde{p}_0}{\tilde{R}}. \quad (11)$$

For the purposes of fitting a circle to the observed orbital planes (q_i, p_i) , we assume that the observed planes are the model planes plus random deviations with Gaussian statistics. That is, the observed orbital planes (q_i, p_i) are related

²¹⁸ to the model orbital planes $(\tilde{q}_i, \tilde{p}_i)$ as

$$q_i = \tilde{q}_i + \tilde{\delta}_i, \quad p_i = \tilde{p}_i + \tilde{\varepsilon}_i, \quad (12)$$

²¹⁹ with $(\tilde{\delta}_i, \tilde{\varepsilon}_i)$ an isotropic bivariate Gaussian random variable with zero mean and a model variance in each direction of $\tilde{\sigma}^2$.

²²¹ The least-squares circle fit minimizes the sum of squares for the projected distances from the observed points to
²²² the model (fitted) circle. If we write the estimated center and radius as $\hat{\Theta} = (\hat{q}_0, \hat{p}_0, \hat{R})$ and the model center and radius
²²³ as $\tilde{\Theta} = (\tilde{q}_0, \tilde{p}_0, \tilde{R})$, then $\hat{\Theta}$ is found as

$$\hat{\Theta} = \operatorname{argmin} \left[\sum_{i=1}^n \left(\sqrt{(q_i - \hat{q}_0)^2 + (p_i - \hat{p}_0)^2} - \hat{R} \right)^2 \right], \quad (13)$$

²²⁴ where the argmin function refers to the values of $(\hat{q}_0, \hat{p}_0, \hat{R})$ that result in the smallest value of Θ . The specific numerical
²²⁵ method used for the minimization is not important to this paper. To leading order, the least-squares circle fit has zero
²²⁶ bias in q_0 and p_0 . The small bias in R is not important to this paper, as we are only concerned with the location of the
²²⁷ mean plane. To leading order, the covariance matrix of the fit is

$$E[(\hat{\Theta} - \tilde{\Theta})(\hat{\Theta} - \tilde{\Theta})^T] = \tilde{\sigma}^2(\tilde{\mathbf{W}}^T \tilde{\mathbf{W}}^{-1}), \quad (14)$$

²²⁸ where $\tilde{\sigma}^2$ is the model variance of the Gaussian noise and

$$\tilde{\mathbf{W}} = \begin{bmatrix} \tilde{u}_1 & \tilde{v}_1 & 1 \\ \vdots & \vdots & \vdots \\ \tilde{u}_n & \tilde{v}_n & 1 \end{bmatrix}. \quad (15)$$

²²⁹ Because we do not know the model values of $(\tilde{u}_i, \tilde{v}_i)$ to compute $\tilde{\mathbf{W}}$, we compute an approximate version $\hat{\mathbf{W}}$ using

$$\hat{u}_i = \frac{q_i - \hat{q}_0}{\hat{R}}, \quad (16)$$

$$\hat{v}_i = \frac{p_i - \hat{p}_0}{\hat{R}}. \quad (17)$$

²³⁰ Because we do not know the model value of $\tilde{\sigma}^2$, we compute

$$\hat{\phi}_i = \arctan(p_i - \hat{p}_0, q_i - \hat{q}_0), \quad (18)$$

²³¹

$$\hat{q}_i = \hat{q}_0 + \hat{R} \cos \hat{\phi}_i, \quad (19)$$

$$\hat{p}_i = \hat{p}_0 + \hat{R} \sin \hat{\phi}_i, \quad (20)$$

$$\hat{\delta}_i = q_i - \hat{q}_i, \quad (21)$$

$$\hat{\varepsilon}_i = p_i - \hat{p}_i. \quad (22)$$

²³² We then calculate an approximate noise variance $\hat{\sigma}^2$ as the variance of the $\hat{\delta}_i$ and the $\hat{\varepsilon}_i$. This is not rigorously justified,
²³³ but it aligns with the use of the known sample variance instead of the unknown population variance when calculating
²³⁴ confidence intervals for ordinary Gaussian distributions.

²³⁵ Thus our estimated covariance matrix for the circle fit is

$$\hat{E}[(\hat{\Theta} - \tilde{\Theta})(\hat{\Theta} - \tilde{\Theta})^T] = \hat{\sigma}^2(\hat{\mathbf{W}}^T \hat{\mathbf{W}}^{-1}) \quad (23)$$

²³⁶ or

$$\hat{E}[\cdot] = \begin{bmatrix} \hat{\sigma}_{q_0}^2 & \hat{\rho}_{q_0 p_0} \hat{\sigma}_{q_0} \hat{\sigma}_{p_0} & \hat{\rho}_{q_0 R_0} \hat{\sigma}_{q_0} \hat{\sigma}_{R_0} \\ \hat{\rho}_{q_0 p_0} \hat{\sigma}_{q_0} \hat{\sigma}_{p_0} & \hat{\sigma}_{p_0}^2 & \hat{\rho}_{p_0 R_0} \hat{\sigma}_{p_0} \hat{\sigma}_{R_0} \\ \hat{\rho}_{q_0 R_0} \hat{\sigma}_{q_0} \hat{\sigma}_{R_0} & \hat{\rho}_{p_0 R_0} \hat{\sigma}_{p_0} \hat{\sigma}_{R_0} & \hat{\sigma}_{R_0}^2 \end{bmatrix}, \quad (24)$$

where $\hat{\sigma}_{q_0}$ is the ordinary Gaussian standard deviation of the estimate for q_0 , $\hat{p}_{q_0 p_0}$ is the correlation coefficient between the estimate for q_0 and the estimate for p_0 , etc.

Later, when analyzing the orbit poles of the **Hilda, Schubart, Potomac, and Ismene clones as seen in Figure 4**, we adopt one-dimensional 95% confidence intervals for the location of the circle-fit mean plane as $\hat{q}_0 \pm 1.96\hat{\sigma}_{q_0}$, $\hat{p}_0 \pm 1.96\hat{\sigma}_{p_0}$. This is in accordance with the interval for symmetric 95% probability mass around the mean of a univariate standard normal distribution.

4. The Hilda Asteroids

The asteroids in Jupiter's interior 3:2 MMR are known as the Hilda group, after asteroid Hilda. For this study, we used the lists of the 6393 Hilda asteroids and their collisional families provided by Vokrouhlický, Nesvorný, Brož, Bottke, Deienno, Fuls and Shelly (2025). The asteroids in the lists by Vokrouhlický et al. (2025) occupy a semimajor axis range of 3.80–4.16 au. Using code from (Hendler and Malhotra, 2020), we estimate for them an observational completeness limit of absolute magnitude $H \leq 16.3$. That is, to a good approximation, every object with $H \leq 16.3$ has been observed. At the time of this study, the observationally complete sample size is nearly 4000. This large sample size makes the Hilda group the best candidate for studying the dynamics of the mean plane of a group of resonant objects. Other potential candidate groups present much smaller observationally complete sample sizes or require a large amount of delicate work to mitigate observational biases to construct a model population.

Within their list of the Hilda group asteroids, Vokrouhlický et al. (2025) reported several collisional families. They identified these collisional families by using hierarchical clustering analysis of the asteroids' proper elements obtained by means of a fully numerical method; for details, the reader is referred to Vokrouhlický et al. (2025, Appendix C). As alluded to in section 3.1, there are three prominent collisional families. These are named after the their parent asteroids Hilda, Schubart, and Potomac, and we call them the "Hilda family", "Schubart family", and "Potomac family" to contrast them with the "background Hildas" in no collisional family and the "Hilda group" that includes all asteroids in Jupiter's interior 3:2 MMR. The Hilda and Schubart families were previously identified by Brož et al. (2011); Schubart (1982a,b). There are three other small collisional families named after their parent asteroids 2008 TG106, Guinevere, and Francette (Vokrouhlický et al., 2025).

Among the 6393 Hilda group asteroids, Vokrouhlický et al. (2025) report 1066 objects in the Hilda family, 1882 in the Schubart family, 506 in the Potomac family, 151 in the Francette family, 54 in the Guinevere family, and 17 in the 2008 TG106 family. However, all but one object in the 2008 TG106 family is also in the Schubart family, so we assign the remaining object to the background Hildas and do not consider the 2008 TG106 family any more.

Starting with this dataset, we used Astroquery in Python to download H magnitudes and osculating heliocentric elements in the J2000 ecliptic frame for each object from the JPL Horizons web service (JPL Solar System Dynamics Group, 2024). The orbital elements and H magnitudes used an epoch of JD 2460796.5, or 1 May 2025 00:00:00. We used the Python code provided by Hendler and Malhotra (2020) to obtain an observational completeness limit of $H \leq 16.3$ for the objects listed by Vokrouhlický et al. (2025), and then we selected all 3893 objects brighter than that limit.

In our sample of 3893 asteroids with $H \leq 16.3$, there are 737 in the Hilda family, 983 in the Schubart family, 359 objects in the Potomac family, 52 in the Francette and Guinevere families, and 1762 background Hildas. Because of the small numbers in the Francette and Guinevere families, we do not discuss these families further in this work.

Figure 2a shows scatter plots of the osculating heliocentric orbital elements as of May 1, 2025 for our observationally complete sample of the Hilda group. For the group as a whole, we observe that the semimajor axis and eccentricity are uncorrelated. For each of the collisional families, we observe that the inclination is sharply bounded, and that the semimajor axis and eccentricity are randomly distributed within ranges that are smaller for the higher inclination families. The osculating heliocentric orbital planes as of May 1, 2025 are plotted in q and p in Figure 2b, with the Hilda, Schubart, and Potomac families respectively highlighted in red, blue, and goldenrod. The collisional families appear as three distinct annular rings that are nearly uniformly distributed around their centers. We will interrogate this uniform appearance later.

It should be noted that collisional families could, in principle, present as an arc if the family were young enough that the orbital planes were not sufficiently differentially precessed to uniformly fill a ring. This is not the case with the Hilda, Schubart and Potomac families. According to Milani, Knežević, Spoto, Cellino, Novaković and Tsirvoulis (2017), the Schubart family is roughly 1.6 Gyr old, while the Hilda family is about 5.0 Gyr old. The timescale to turn a short arc into a nearly uniform ring depends inversely on the initial semimajor axis dispersion. For reference, we

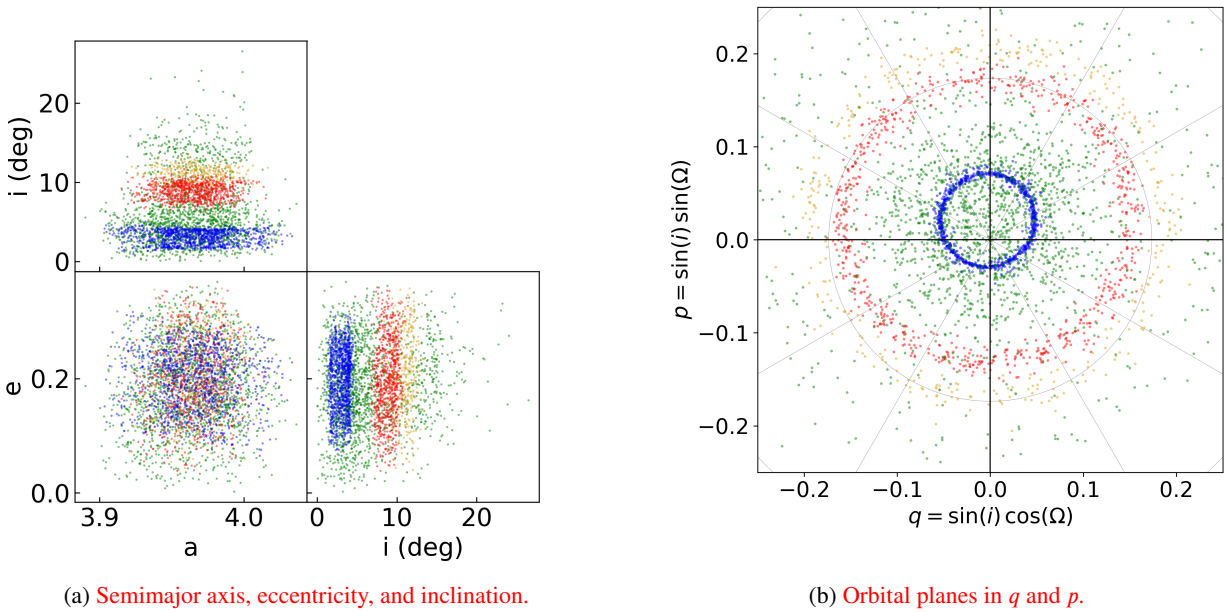


Figure 2: Heliocentric osculating orbital elements in the J2000 ecliptic frame for the observationally-complete Hilda-group asteroids with absolute magnitude $H \leq 16.3$ as of May 1, 2025. The collisional Hilda, Schubart, and Potomac families are respectively colored red, blue, and goldenrod. All other objects are colored green.

288 find from numerical integrations that the timescale for a young collisional family to differentially precess and fill out a
 289 ring in q and p is a few hundred kyr, if each object in the family begins with the same orbital plane and an osculating
 290 semimajor axis dispersion of ± 0.01 au from the parent body. A wider semimajor axis dispersion of ± 0.1 au, similar to
 291 that observed for the collisional families, can be expected to fill out a ring in q and p in a shorter time, on the order of
 292 tens of kyr.

293 5. The Mean Plane of the Hildas Today

294 Following the methods described in Section 3.1, we computed the sample mean plane $\hat{\mathbf{q}}_0$ and its uncertainty angles
 295 $\phi_{68\%}$, $\phi_{95\%}$, and $\phi_{99.7\%}$ for the Hilda group as a whole, and for the collisional Hilda, Schubart, and Potomac families
 296 taken separately.

297 Figure 3 displays the sample mean planes and their 68%, 95%, and 99.7% confidence regions for each of the three
 298 groups on May 1, 2025. In these plots, we label the sample mean planes $\hat{\mathbf{q}}_0$ of the Hilda, Schubart, and Potomac families
 299 as ‘‘H’’, ‘‘S’’, and ‘‘P’’, and we label the sample mean plane of the entire population with $H \leq 16.3$ as ‘‘A’’ for ‘‘all’’.
 300 We label the Laplace plane $\hat{\mathbf{q}}_0$ computed at the mean semimajor axis of the sample as ‘‘L’’ for ‘‘Laplace’’. We label
 301 the orbital plane of Jupiter as ‘‘J’’, and we label the invariable plane of the Solar System as ‘‘I’’. We calculate this by
 302 normalizing the total barycentric orbital angular momentum vector of the Sun and planets in our simulation. Here its
 303 location in the heliocentric J2000 reference frame is $q = -0.00834$, $p = 0.0262$, which is $i = 1.58^\circ$, $\Omega = 107.6^\circ$.

- 304 • Subplot (a) shows the mean plane uncertainty for the entire Hilda group. The Jupiter plane, forced plane, and
 305 Schubart plane are within the 68% region, while the Hilda family plane, Potomac plane, and invariable plane are
 306 outside the 99.7% region.
- 307 • Subplot (b) shows the mean plane uncertainty for the Hilda family. The Jupiter plane, forced plane, Hilda group
 308 plane, and Schubart plane are within the 95% region, and the Potomac plane and invariable plane are within the
 309 99.7% region.

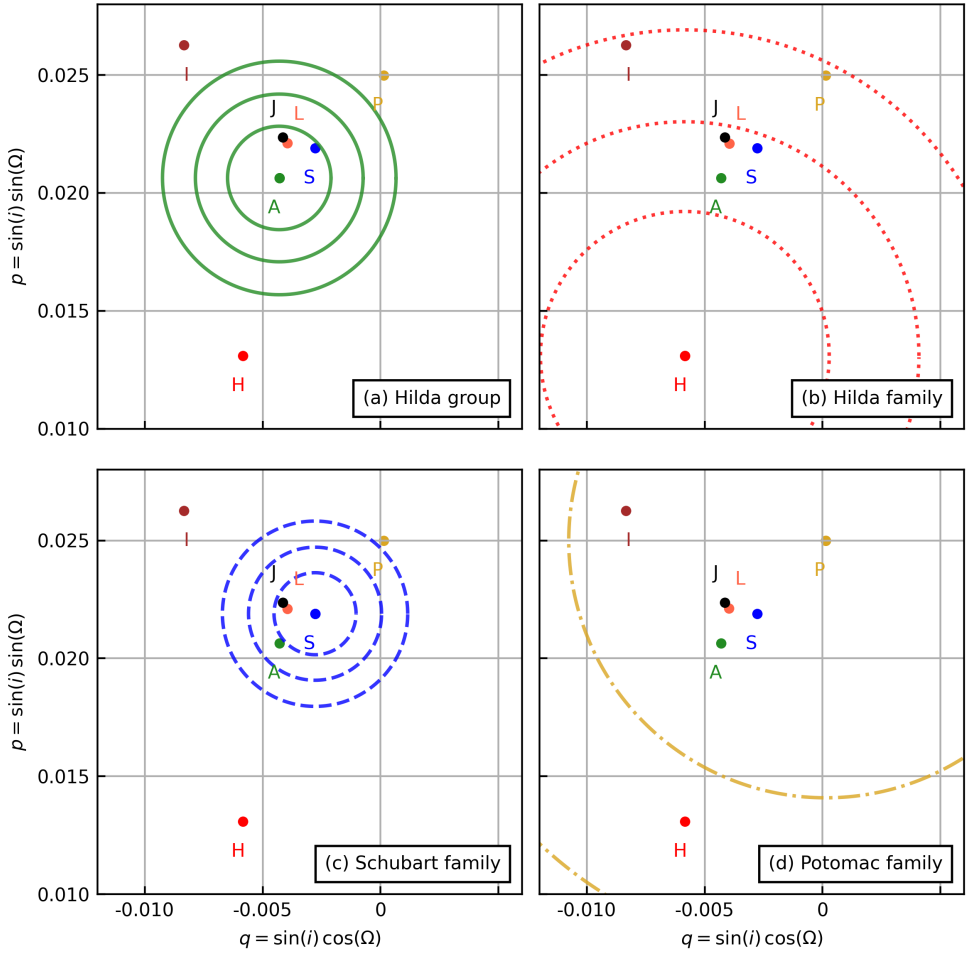


Figure 3: The present-day sample mean planes and their uncertainty regions. Each subplot contains the invariable plane (purple, I), the Jupiter plane (black, J), the Laplace plane (orange, L), the Hilda group mean plane (green, A), the Hilda family mean plane (red, H), the Schubart family mean plane (blue, S), and the Potomac family mean plane (goldenrod, P), as well as the 68%, 95%, and 99.7% uncertainty regions for the sample mean of the population labeled in the bottom-right corner. Note that this figure is contained well inside the ring of blue dots in Figure 2b, and this figure does not show the orbital planes of individual asteroids. In subplot (d), only the 68% and 95% uncertainty regions are shown.

- 310
- 311 • Subplot (c) shows the mean plane uncertainty for the Schubart family. The Jupiter plane, forced plane, and Hilda group plane are within the 95% region, and the Hilda family plane, Potomac plane, and invariable plane are outside the 99.7% region.
 - 312
 - 313 • Subplot (d) shows the mean plane uncertainty for the Potomac family. All other planes are within the 95% region.
 - 314

315 We call two planes statistically indistinguishable if either plane is within the 95% uncertainty region of the other
 316 plane. Figure 3 shows that it is statistically plausible that each collisional family has the same mean plane as every
 317 other collisional family and the entire Hilda group, and we have no dynamical reason to suspect otherwise. In each
 318 case, the mean plane is statistically indistinguishable from the Laplace plane or from the orbital plane of Jupiter, which
 319 is nearly identical to the Laplace plane. However, the Hilda-group mean plane and the Schubart-family mean plane
 320 are statistically distinct from the invariable plane of the Solar System. Dynamically speaking, if we do not identify the
 321 Hilda-group or Schubart-family mean planes with the invariable plane, we have no reason to identify the Hilda-family
 322 or Potomac-family mean planes with the invariable plane either. The larger uncertainty regions for the Hilda-family

Category	n	i_0	Ω_0	$\phi_{95\%}$
Hilda group	3893	1.21°	101.8°	0.20°
Hilda family	737	0.82°	114.0°	0.57°
Schubart family	983	1.26°	97.2°	0.16°
Potomac family	359	1.43°	89.7°	1.01°

Table 2

Mean plane locations of the Hilda group, Hilda family, Schubart family, and Potomac family, in degrees, relative to the ecliptic plane. Columns are category; object count ($H \leq 16.3$); inclination and ascending node of the mean plane; and the half-angle $\phi_{95\%}$ for the 95% uncertainty region.

and Potomac-family mean planes are due to the higher average relative inclinations of the Hilda and Potomac families, as shown in Figure 1.

The numerical values of the current mean planes of each population are given in Table 2. The mean inclination for the Hilda family of $i_0 = 0.82^\circ \pm 0.57^\circ$ compares favorably with the Vinogradova (2015) result of $i_0 = 1.20^\circ \pm 0.05^\circ$, but the mean longitude of ascending node $\Omega_0 = 114.0^\circ \pm 0.57^\circ$ is far from the Vinogradova (2015) result of $\Omega_0 = 99^\circ \pm 1^\circ$.

6. The Mean Plane of the Hildas Over Time

We have shown that, at the present time, the mean planes of the Hilda group and its three collisional families are statistically indistinguishable from each other, and their mean plane statistically indistinguishable from the Laplace plane or the orbital plane of Jupiter. We have also shown that the invariable plane is statistically distinct from the mean plane of the Hilda group or the Schubart family. However, it is conceivable that this observation at the present time is a statistical fluctuation rather than the true state of things. To show that this observation is dynamically meaningful, we must see whether it persists over secular timescales, and we must check that it applies to individual objects as well as to observed populations.

We used the WHFAST integrator in REBOUND (Rein and Liu, 2012) to integrate the giant planets and the Hilda-group asteroids for 2 Myr, with a step size of 0.2 yr and an output cadence of 200 yr. The solar mass in these integrations was augmented by the total mass of the terrestrial planets, and the mass ratios of the giant planets relative to the Sun were reduced proportionately. We also chose one member of each population to examine individually, generated 500 clones based on each of the chosen objects, and integrated those clones for 2 Myr with the same step size and output cadence. We chose asteroid Hilda to represent the Hilda family, asteroid Schubart to represent the Schubart family, asteroid Potomac to represent the Potomac family, and asteroid Ismene to represent Hilda-group asteroids in no collisional family. Each clone used the orbital elements of the observed asteroid, plus a semimajor axis displacement drawn from the uniform random distribution on $[-0.01, 0.01]$ au. Our use of a uniform initial semimajor axis distribution for the clones, with constant initial inclination and eccentricity, is justified by the uniform semimajor axis distributions of the collisional families seen in Figure 2a, together with the lack of correlation between semimajor axis and eccentricity. The width of the semimajor axis dispersion was chosen to keep all clones well within the semimajor axis range of Jupiter's interior 3:2 MMR. We found by numerical experimentation that increasing the semimajor axis dispersion of the clones by an order of magnitude could result in some clones exhibiting chaotic evolution, which is unsuitable for our purpose. The results of these integrations are shown in Figures 4–5.

Figure 4 shows the difference in $q = \sin i \cos \Omega$ between the sample mean plane and two reference planes. The left column shows this difference for the Hilda group and the Hilda, Schubart, and Potomac families, and the right column shows it for the clones of Ismene, Hilda, Schubart, and Potomac. The difference between the sample mean plane and the invariable plane is shown in green, and the difference between the sample mean plane and the Laplace plane is shown in blue. The difference between the sample mean plane and the Jupiter plane is nearly identical to the difference between the sample mean and the Laplace plane, so it is omitted. The 95% confidence limits for the location of the mean plane in q are shown in black. The same plot in p looks very similar, and is omitted. In every case except the Potomac family, the difference between the sample mean and the invariable plane is too large to be accommodated within the 95% uncertainty limits, while the difference between the sample mean and the Laplace plane is not. Because the Potomac family has a higher inclination and a smaller sample size than the Hilda family and the Schubart family, its 95% uncertainty interval is large enough to enclose the invariable plane.

Figure 5 shows the angular distance, in degrees, between the sample mean planes of the various populations and the invariable plane, the orbital plane of Jupiter, and the Laplace plane. The left column shows this distance for the Hilda group and the Hilda, Schubart, and Potomac families, and the right column shows it for the clones of Ismene, Hilda, Schubart, and Potomac. The black trace is the distance between the sample mean and the invariable plane, the blue trace is the distance between the sample mean and the Jupiter plane, and the red trace is the distance between the sample mean and the Laplace plane. In the left column, the data has been smoothed over a moving average of 50 kyr to make the differences between the traces easier to see. In each case, the invariable plane is substantially farther from the sample mean plane than the Jupiter plane is, and the Jupiter plane is slightly farther from the sample mean than the Laplace plane is.

7. Summary and Discussion

The present investigation was motivated by curiosity to know the forced orbital plane of resonant groups of small bodies in the solar system, as this is not addressed in the literature. We chose the observationally complete ($H \leq 16.3$) set of Hilda asteroids for this investigation. This dynamical group librates in Jupiter's interior 3:2 mean motion resonance, and its sample size is nearly 4000.

From the observational data, we measured the mean planes of the Hilda group and the collisional families therein, as well as the uncertainties of these measurements. Table 2 shows that the orientation of the present-day mean plane of the Hilda group can be measured to an accuracy of 0.2° , and the mean planes of the Hilda family, Schubart family, and Potomac family can respectively be measured to accuracies of 0.57° , 0.16° , and 1.01° .

We found that the 95% uncertainty region of the sample mean plane of the Hilda group encompasses both Jupiter's current orbital plane as well as the instantaneous forced plane predicted by the Laplace-Lagrange linear secular theory for the average semimajor axis of the Hilda group, but it does not enclose the invariable plane.

Furthermore, with N -body numerical simulation for 2 Myr, we found that the motion of the sample mean plane of the Hilda group continues to track the Laplace plane, but not the invariable plane. Because the Laplace plane in the Hilda region is nearly identical to the Jupiter plane, we cannot distinguish between the Laplace plane and the orbital plane of Jupiter as hypotheses for the true forced plane of the Hilda asteroids.

We tentatively qualitatively explain this result as follows. Because the Hilda group is in closer proximity to Jupiter and the other giant planets are much farther away and of lower mass, the dynamical environment can be closely approximated by the restricted three-body problem with the Sun, Jupiter, and a massless small body. In the restricted three-body problem, the instantaneous forced plane is expected to be identical to the Jupiter plane; there is no other preferred plane around which a massless small body's orbital plane can precess. In the less restricted problem with additional planets on non-coplanar orbits, there are four possible hypotheses for the forced plane: the invariable plane, Jupiter's orbital plane (if Jupiter dominantly controls the dynamics of the resonant population), the Laplace plane, or one that is distinct from all of these if the mean motion resonance strongly affects the forced plane dynamics of resonant populations. Our results rule out the invariable plane as the forced plane of the Hilda group at high statistical confidence. However, the present-day observationally complete sample size cannot distinguish between the second and third of these hypotheses for three reasons: the size of the sample, its significant inclination dispersion, and the nearness of the Laplace plane to the Jupiter plane.

Our study's main weakness is the lack of a rigorous procedure to quantify the statistical plausibility of a reference plane as the true forced plane over time, as opposed to its statistical plausibility as the true mean plane at any instant of time. Because the separation between the instantaneous Laplace plane and Jupiter's orbital plane is so small, it will be necessary to dramatically increase the sample size to clearly distinguish between the two of them as potential true forced planes for the Hilda asteroids. In the last five years the observational completeness limit for the Hilda group has been pushed from $H \leq 15.7$ (Hendler and Malhotra, 2020) to $H \leq 16.3$, increasing the observationally complete sample size from 2111 to 3893. In the future the Vera C. Rubin Observatory and other powerful telescopes may push the observational completeness limit to fainter magnitudes, increasing the sample size enough to permit a more precise measurement of the mean plane of the Hilda asteroids and a more sensitive investigation of its dynamics. Future studies might also investigate whether unseen distant perturbers can warp the linear secular forced plane enough to account for the time-varying differences between it and the mean plane of the Hilda group, but we have little *a priori* reason to expect that a large, distant unseen planet would have a dramatic effect on the orbital planes of small bodies so close to Jupiter.

413 8. Data Availability

414 The initial orbital elements for the planets and Hilda asteroids, as well as our Python code, are available for
 415 download from https://github.com/iwygh/mm25_hildas.

416 9. Acknowledgments

417 Funding for IM was provided by NASA FINESST grant 80NSSC23K1362. We gratefully acknowledge the
 418 thoughtful reviews from Matt Clement and the anonymous reviewer.

419 CRediT authorship contribution statement

420 **Ian C. Matheson:** Investigation, Formal analysis, Software, Visualization, Data curation, Writing - original draft,
 421 Writing - review & editing. **Renu Malhotra:** Conceptualization, Funding acquisition, Supervision, Writing - review
 422 & editing.

423 References

- 424 Al-Sharadqah, A., Chernov, N., 2009. Error analysis for circle fitting algorithms. *Electronic Journal of Statistics* 3, 886–911.
- 425 Brož, M., Vokrouhlický, D., Morbidelli, A., Nesvorný, D., Bottke, W., 2011. Did the hilda collisional family form during the late heavy
 426 bombardment? *Monthly Notices of the Royal Astronomical Society* 414, 2716–2727.
- 427 Chiang, E., Choi, H., 2008. The warped plane of the classical kuiper belt. *The Astronomical Journal* 136, 350. doi:[doi:10.1088/0004-6256/136/1/350](https://doi.org/10.1088/0004-6256/136/1/350).
- 428 Dahlgren, M., Lagerkvist, C.I., Fitzsimmons, A., Williams, I., Gordon, M., 1997. A study of hilda asteroids. ii. compositional implications from
 429 optical spectroscopy. *Astronomy and Astrophysics*, v. 323, p. 606-619 323, 606–619.
- 430 Ferraz-Mello, S., Michtchenko, T., Nesvorný, D., Roig, F., Simula, A., 1998. The depletion of the hecuba gap vs the long-lasting hilda group.
 431 Planetary and Space Science 46, 1425–1432. URL: <https://www.sciencedirect.com/science/article/pii/S0032063398000233>,
 432 doi:[https://doi.org/10.1016/S0032-0633\(98\)00023-3](https://doi.org/10.1016/S0032-0633(98)00023-3). second Italian Meeting on Celestial Mechanics.
- 433 Franklin, F.A., Lewis, N.K., Soper, P.R., Holman, M.J., 2004. Hilda asteroids as possible probes of jovian migration. *The Astronomical Journal*
 434 128, 1391.
- 435 Henderl, N.P., Malhotra, R., 2020. Observational completion limit of minor planets from the asteroid belt to jupiter trojans. *The Planetary Science
 436 Journal* 1, 75.
- 437 JPL Solar System Dynamics Group, 2024. Horizons system. <https://ssd.jpl.nasa.gov/horizons/>. Accessed: 2024-04-23.
- 438 Klearn, M., Lauritzen, M.E., 2023. circle-fit: A circle-fitting library for python. URL: <https://github.com/AlliedToasters/circle-fit>.
- 439 Knezević, Z., Lemaître, A., Milani, A., 2002. The Determination of Asteroid Proper Elements. *Asteroids III*, 603–612.
- 440 Matheson, I., Malhotra, R., 2023. A measurement of the kuiper belt's mean plane from objects classified by machine learning. *The Astronomical
 441 Journal* 165, 241.
- 442 Matheson, I.C., Malhotra, R., Keane, J.T., 2023. A von mises–fisher distribution for the orbital poles of the plutinos. *Monthly Notices of the Royal
 443 Astronomical Society* 522, 3298–3307.
- 444 Milani, A., Knežević, Z., Spoto, F., Cellino, A., Novaković, B., Tsirvoulis, G., 2017. On the ages of resonant, eroded and fossil asteroid families.
 445 *Icarus* 288, 240–264.
- 446 Morbidelli, A., 1993. Asteroid secular resonant proper elements. *Icarus* 105, 48.
- 447 Morbidelli, A., Moons, M., 1993. Secular resonances in mean motion commensurabilities: the 2/1 and 3/2 cases. *Icarus* 102, 316–332.
- 448 Murray, C.D., Dermott, S.F., 1999. *Solar System Dynamics*. Cambridge University Press.
- 449 Nesvorný, D., Ferraz-Mello, S., 1997. On the asteroidal population of the first-order jovian resonances. *Icarus* 130, 247–258.
- 450 Nesvorný, D., Roig, F., Vokrouhlický, D., Brož, M., 2024. Catalog of proper orbits for 1.25 million main-belt asteroids and discovery of 136 new
 451 collisional families. *The Astrophysical Journal Supplement Series* 274, 25.
- 452 Rein, H., Liu, S.F., 2012. REBOUND: an open-source multi-purpose N-body code for collisional dynamics. *Astron. & Astrophys.* 537, A128.
 453 doi:[10.1051/0004-6361/201118085](https://doi.org/10.1051/0004-6361/201118085), arXiv:1110.4876.
- 454 Schubart, J., 1982a. Numerical determination of proper inclinations of hilda-type asteroids. *Celestial mechanics* 28, 189–194.
- 455 Schubart, J., 1982b. Three characteristic parameters of orbits of hilda-type asteroids. *Astronomy and Astrophysics* 114, 200–204.
- 456 Vinogradova, T., 2015. Identification of asteroid families in trojans and hildas. *Monthly Notices of the Royal Astronomical Society* 454, 2436–2440.
- 457 Vokrouhlický, D., Bottke, W.F., Nesvorný, D., 2016. Capture of trans-neptunian planetesimals in the main asteroid belt. *The Astronomical Journal*
 458 152, 39.
- 459 Vokrouhlický, D., Nesvorný, D., Brož, M., Bottke, W.F., Deienno, R., Fuls, C.D., Shelly, F.C., 2025. Orbital and absolute magnitude distribution
 460 of hilda population. *The Astronomical Journal* 169, 242.
- 461 Volk, K., Malhotra, R., 2017. The curiously warped mean plane of the kuiper belt. *The Astronomical Journal* 154, 62. doi:[10.3847/1538-3881/aa79ff](https://doi.org/10.3847/1538-3881/aa79ff).
- 462 Wong, I., Brown, M.E., 2017. The color–magnitude distribution of hilda asteroids: Comparison with jupiter trojans. *The Astronomical Journal* 153,
 463 69.
- 464 Wong, I., Brown, M.E., Emery, J.P., 2017. 0.7–2.5 μm spectra of hilda asteroids. *The Astronomical Journal* 154, 104.

Hilda asteroids' forced plane

⁴⁶⁷ Zain, P., Di Sisto, R., Gil-Hutton, R., 2025. Collisional study of hilda and quasi-hilda asteroids. *Astronomy & Astrophysics* 694, A298.

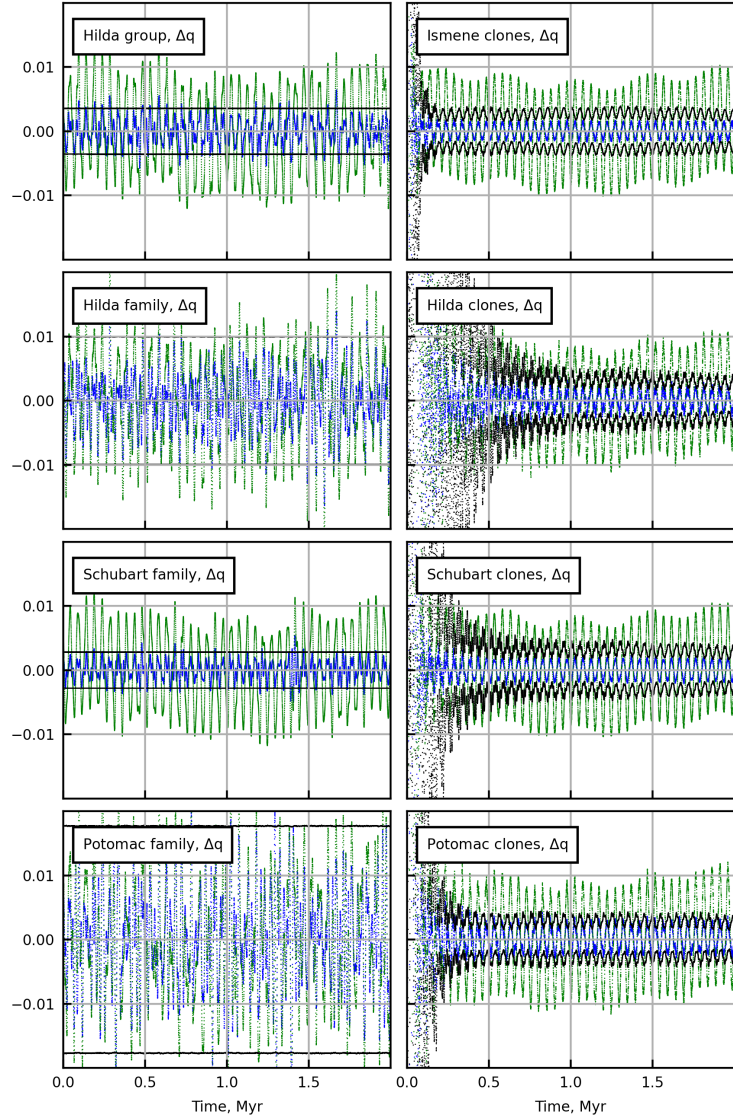


Figure 4: In each panel, the blue trace is the difference, in $q = \sin i \cos \Omega$, between the sample mean plane and the instantaneous Laplace plane. The difference in q between the sample mean plane and the Jupiter plane would appear nearly identical, and is omitted. The black trace is the 95% confidence interval for the mean plane, and the green trace is the difference in q between the sample mean plane and the invariable plane. For nearly every set of observed objects or clones, the Laplace plane falls within the confidence interval for the mean plane, but the invariable plane does not. Because of the Potomac family's higher inclination and smaller sample size, its 95% uncertainty region for the mean plane is large enough to enclose the invariable plane.

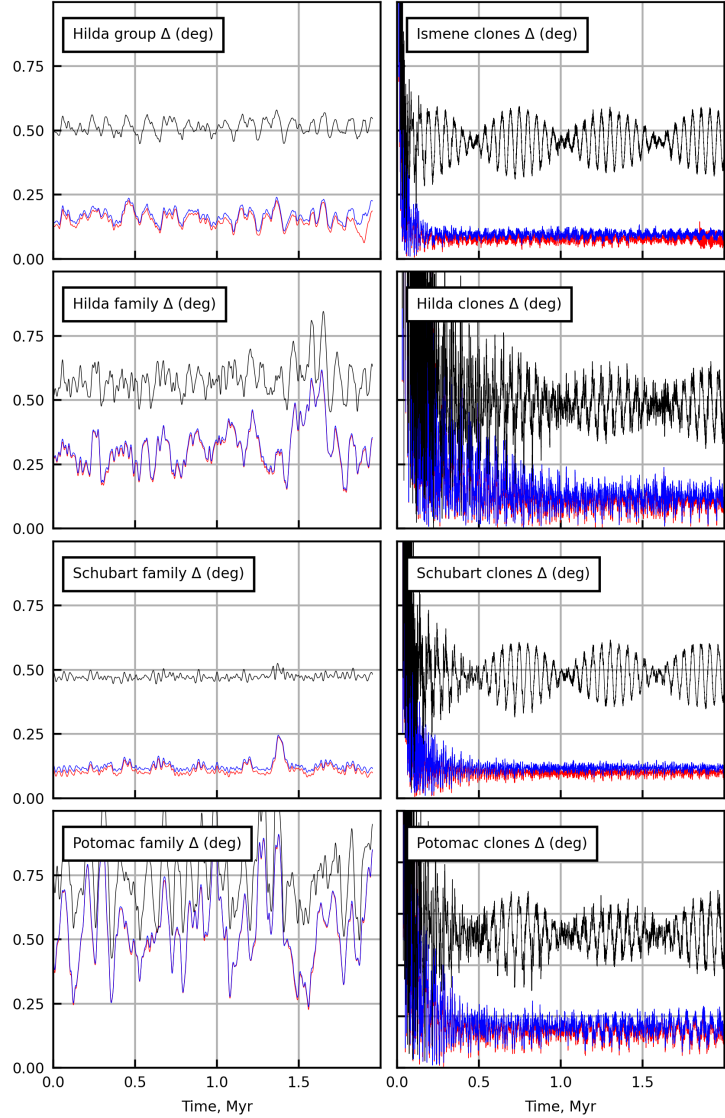


Figure 5: The time-varying angular separation, in degrees, between the mean planes of the indicated groups in each subplot and the invariable plane (black), the orbit pole of Jupiter (blue), and the instantaneous Laplace plane (red). The sets of objects in the various subplots are the Potomac family, 500 clones of asteroid Potomac, the Hilda family, 500 clones of asteroid Hilda, the Schubart family, 500 clones of asteroid Schubart, the background Hildas, 500 clones of asteroid Ismene (a background Hilda), and all members of Jupiter's interior 3:2 MMR. The data in the left column has been smoothed by a running average over 50 kyr to make the differences between the black, red, and blue traces easier to see. In each case, the invariable plane is substantially farther from the sample mean than the Jupiter plane is, and the Jupiter plane is slightly farther from the sample mean than the Laplace plane is.